

Margin Failures in Crown-Like Brittle Structures: Off-Axis Loading

Chris Ford,¹ Tarek Qasim,¹ Mark B Bush,¹ Xiaozhi Hu,¹ Mahek M Shah,² Vibhu P Saxena,² Brian R. Lawn³

¹ School of Mechanical Engineering, The University of Western Australia, Crawley, Western Australia 6009, Australia

² Department of Mechanical Engineering, Indian Institute of Technology, Chennai, India

³ Materials Science and Engineering Laboratory, National Institute of Standards and Technology, Gaithersburg, Maryland 20899-8520

Received 20 March 2007; revised 23 May 2007; accepted 30 May 2007

Published online 14 August 2007 in Wiley InterScience (www.interscience.wiley.com). DOI: 10.1002/jbm.b.30911

Abstract: The effect of off-axis loading of compliant indenters on the initiation of cracks at the margins of dental crown-like dome structures consisting of glass shells back-filled with an epoxy resin is examined. As in previous studies on similar structures but with strictly axial loading, cracks can be made to initiate and propagate from the margins around the dome faces into a “semi-lunar” fracture pattern characteristic of some all-ceramic crown failures. In this study, balsa wood and teflon disk indenters are used to provide the off-axis loading, at 45° to the dome axis. The soft indenters, considered representative of food bolus, spread the contact at the top surface, suppressing otherwise dominant radial cracks that ordinarily initiate at the dome undersurface directly along the load axis beneath harder indenters. Finite element modeling is used to show that off-axis loading dramatically increases the tensile stresses at the near-side dome margin, strongly diminishing the loads required to generate the lunar fracture mode. © 2007 Wiley Periodicals, Inc. * J Biomed Mater Res Part B: Appl Biomater 85B: 23–28, 2008

Keywords: all-ceramic crowns; lunar cracks; crown failure; soft indenters; stress analysis

INTRODUCTION

In recent studies of dome-shaped brittle (glass) shell structures filled with compliant polymers (epoxy resin and polymer composite) and loaded axially with flat disk platens covering a wide range of elastic modulus (metal, dental composite, epoxy, balsa wood), we demonstrated the functionality of several competing failure modes.^{1,2} Such dome structures were considered representative of monolithic ceramic dental crowns on a dentin support in occlusal loading with intervening food bolus. The fracture modes included conventional radial cracking at the dome undersurface and cone cracks at the dome top surface. Most interestingly, these studies revealed the existence of a new mode, margin cracking, starting at the specimen edges and propagating into a characteristic “semi-lunar” or “abfraction” fracture around one side of the dome. Fractures of this type had been reported in the clinical dental literature.^{3–7} These cracks appeared only in contacts with the softest indenters, and at high loads, suggesting that they may occur preferentially in

heavy chewing on soft food. The reason for the shift in fracture origin to the specimen edges was a general suppression of tensile stresses in the vicinity of a spread-out occlusal contact. A necessary precursor for margin failure was the presence of large flaws at the dome edges, for example from grinding or sandblasting in preparation procedures. In summary, margin fractures appeared to be a viable mode of failure, but, in conventional axial loading at least, required uncommonly high loads and exceptionally soft contacts to produce them.

The studies mentioned above were conducted in axial loading, that is with the disk indenter normal to the dome axis. In a separate study using hard spherical indenters on similar dome structures in off-axis loading, such that the contact was still vertical but located at a point on the dome side wall, it was shown that failure could be accelerated by enhancement of radial cracking to the dome edges.⁸ This enhancement came about partly because of a redistribution of tensile stresses within the dome structure, and partly because of a reduction in distance between the contact site and specimen edge. In that study, soft indenters were not used, so that margin failures were not observed. The question now arises as to whether margin fractures will be similarly enhanced in off-axis loading with soft indenters.

In this article we address this question by conducting tests on epoxy-filled glass domes with balsa wood and teflon plas-

Correspondence to: B. R. Lawn (e-mail: brian.lawn@nist.gov)
Contract grant sponsor: National Institute of Dental and Craniofacial Research; Contract grant number: PO1 DE10976
Contract grant sponsor: Australian Research Council

© 2007 Wiley Periodicals, Inc. *This article is a US Government work and, as such, is in the public domain in the United States of America.

tic indenters loaded normally but at a point on the specimen side wall located at 45° to the dome axis. This substantial angular offset is chosen to emphasize the influence of side loading, in accordance with extreme chewing practice. We shall demonstrate that the incidence of margin fracture is greatly enhanced in such loading, both in initiation from the edges and subsequent propagation into a lunar-like failure chip. Stress analysis using finite element modeling (FEM) will be used to support the experimental observations.

EXPERIMENTAL METHOD

Materials and Testing

Dome glass/epoxy bilayer structures were fabricated as previously outlined.^{1,8-10} A schematic of the configuration is shown in Figure 1, showing side-on and undersurface views.

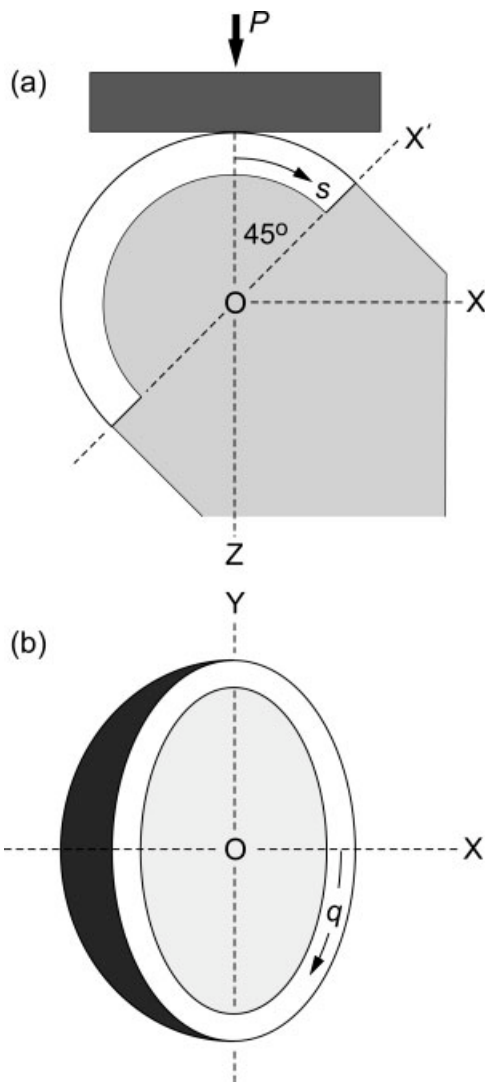


Figure 1. Schematic showing indentation with flat disk on crown-like structure consisting of a brittle hemispherical shell supported by polymeric dentin-like base: (a) side-on view (along OY); (b) undersurface view (along OZ), without substrate. Load is 45° to dome base OX' .

TABLE I. Materials Properties for Input Into FEM

Material	Young's Modulus (GPa)	Poisson's Ratio
Glass	73	0.21
Balsa wood	0.05	0.10
Teflon	0.48	0.35
Epoxy resin	3.4	0.35

Glass plates 1 mm thick (D263, Menze-Glaser, Germany) were shaped into shells of internal radius 6 or 8 mm by slumping over a die at the softening temperature. Hemispherical domes were then prepared by grinding away the base of the glass shells with grade 120 SiC grit paper, and finished by sandblasting the edges and inner surfaces to introduce a uniform density of edge flaws. This was done with sufficient care as to preclude any premature margin crack initiation. All specimens were pre-examined to ensure that they were free of any such precursor cracks.

The shells were then fitted into molds of the same diameter as the shells, hemispherical protrusion outward, and epoxy resin (R2512, ATL Composites, Australia) poured into the mold, layer by layer, with additional cylindrical support bases of depth 10 mm added below the dome rims. The base supports were then machined so as to leave a flat base normal to the prospective 45° loading axis. The specimen bases were then glued to the test platen so as to avoid any lateral slippage of the specimen during subsequent off-axis testing. Loading was carried out using disk indenters of fixed diameter and thickness 10 mm. Two ultra-soft indenter materials were selected: balsa wood and PTFE teflon (E-PLAS Pty. Ltd., Australia). Ultra-soft balsa wood was chosen because of its use in a preceding study,¹ teflon in order to examine a material with modulus intermediate between balsa and crown veneer. Properties of the materials used in the present study are shown in Table I.

The disk indenters were mounted into the cross beam of a mechanical testing machine (Instron 4301, Instron Corp., Canton, MA) and loads applied vertically up to 2000 N at a monotonic rate $\approx 10 \text{ N s}^{-1}$ in air. Crack evolution in the glass domes was monitored *in situ* using a video camera (TRV33E, Sony Corp., Japan), with diffuse lighting behind the specimen to enhance visualization. Because of engulfment of the top surface regions by the softer deforming indenters (especially balsa), such visualization usually had to be augmented by periodically stopping the tests and photographing the specimen independently. These specimens could be replaced on the test stage and loading resumed.

Finite Element Modeling

A finite element algorithm described earlier was adapted to the configuration in Figure 1 to determine the stress distributions.⁹⁻¹¹ Meshing in the critical region between the contact and dome edge was refined, as before, until the stress solutions attained convergence. The deformation was assumed to be elastic everywhere over the load ranges covered. Values

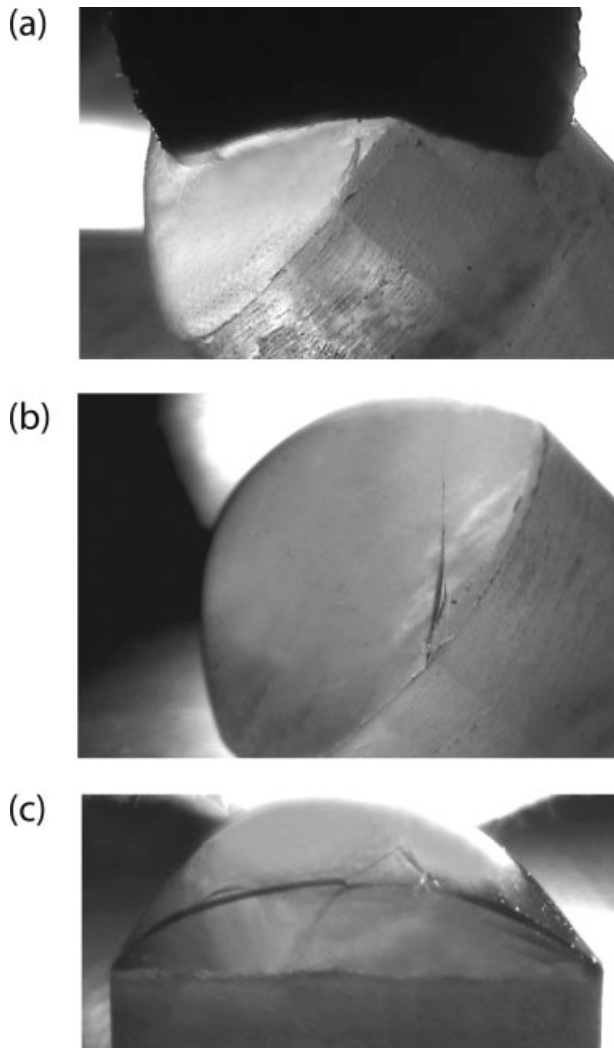


Figure 2. Contact fracture of epoxy-filled glass domes of inner radius 8 mm and thickness 1 mm on epoxy base, indented with balsa wood disk at loads (a) 1000 N (viewed along OY, Figure 1), (b) 1500 N (along OY) and (c) 1800 N (along OX'). Views in (b) and (c) taken after interrupting test. Note how cracks initiate at margin and propagate around side of dome to link up and form 'semi-lunar' chip.

of Young's modulus and Poisson's ratio used in the calculations are listed in Table I. Maximum principal stresses and their directions of action within the dome structures were calculated at each load step, with special attention to distributions along the inner dome surface as a function of longitudinal and latitudinal coordinates s and q in Figure 1.

RESULTS

Experiments

Figure 2 shows margin crack patterns produced in glass domes using off-axis loading with balsa wood disks, as depicted in Figure 1. The photographs are from interrupted tests, at loads (a) 500 N (viewed along OY in Figure 1), (b) 1500 N (same view), and (c) 1800 N (along OX'). In these tests the crack was difficult to follow *in situ*, owing to

engulfment of the contact zone by the soft balsa [Figure 2(a)]. Nevertheless, interrupted views [Figs. 2(b,c)] are sufficient to determine the essence of the evolution. Prior to loading, no cracking was evident in the specimen, including at the margins. During loading, a small crack was observed to pop in from the margin on the near side of the specimen, Figure 2(a). A similar, symmetrically disposed small crack was observed on the back side of the specimen [not visible in Figure 2(a)]. On increasing the load, the cracks propagated upward further toward the contact center, Figure 2(b). Still further load increase caused the cracks on opposite sides of the specimen to link up to form a closed fracture, as seen front-on in Figure 2(c). This is the lunar fracture pattern previously described for axial loading,¹ but now formed without the need for a precursor crack.

Figure 3 shows further examples of margin cracking from off-axis indentation with (a) a balsa disk at load 1000 N (viewed along OY in Figure 1) and (b) a teflon disk at 2000 N (viewed closely parallel to OY). In both cases the cracks have initiated at the edges and have propagated toward the

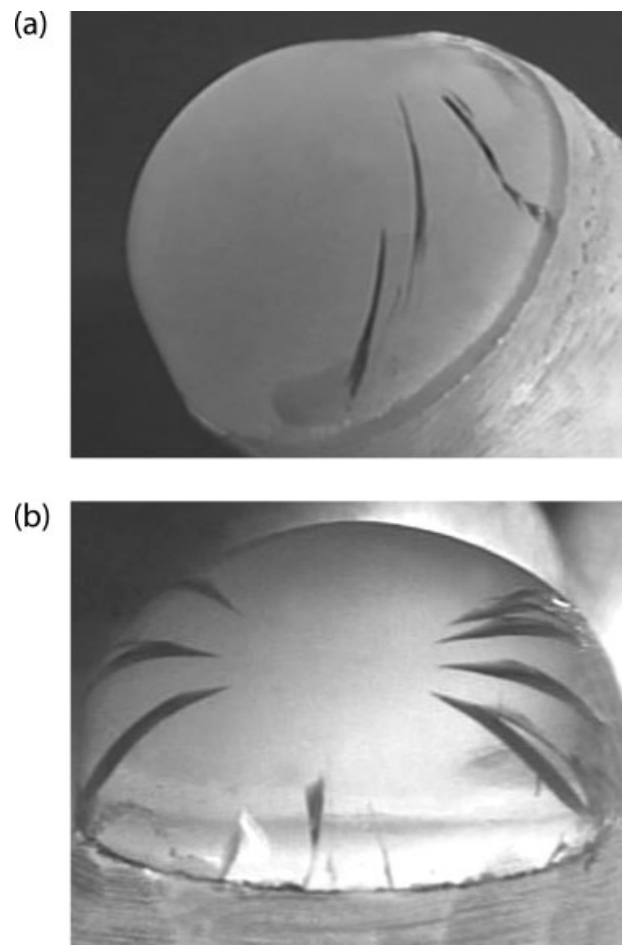


Figure 3. Contact fracture of epoxy-filled glass domes of inner radius 8 mm and thickness 1 mm on epoxy base, indented with (a) balsa disk at load 1000 N (viewed along OY) and (b) teflon disk at 2000 N (closely along OX'). Views taken after interrupting test. Note how margin cracks initiate propagate around side of dome toward contact center.

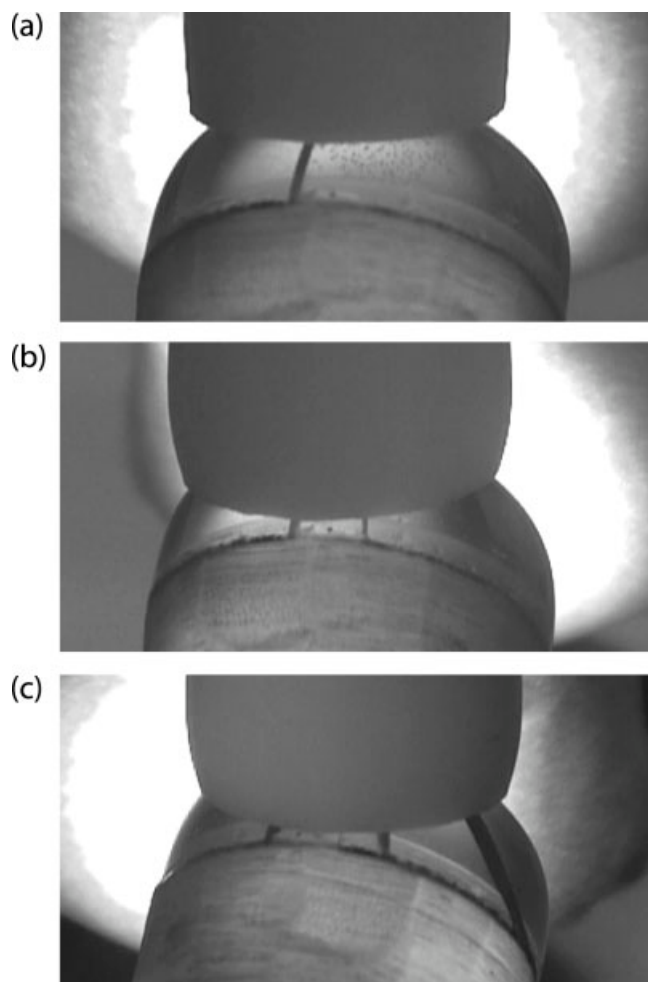


Figure 4. Contact fracture of epoxy-filled glass domes of inner radius 6 mm and thickness 1 mm on epoxy base, indented with teflon disk at loads (a) 630 N, (b) 1360 N, and (c) 1440 N. Views taken *in situ* during loading (closely along OX). Multiple margin cracks are observed.

contact center. It is of interest that these cracks tended to initiate more or less symmetrically on opposite sides of the dome base. The location of such cracks varied from test to test, sometimes closer to the mirror symmetry plane of the loaded dome, but always on the same side face as the contact center. Multiple cracking occurred at higher loads, for example Figure 3(b) relative to Figure 3(a).

A sequence of photographs in Figure 4 shows near-front-on views (closely parallel to OX) of fracture evolution in a teflon-loaded dome at off-axis loads (a) 630 N, (b) 1360 N, and (c) 2000 N. Here the comparatively stiffer teflon indenter (i.e., relative to balsa) allows direct visualization of the cracks during loading, despite heavy deformation of the indenter at the higher loads. In this case the first crack has initiated from the near edge close to the symmetry plane [Figure 4(a)], followed subsequently by two other, symmetrically disposed cracks [Figure 4(b)], and finally additional side cracks [Figure 4(c)].

No radial or cone cracks were observed with the soft balsa indenters up to 2000 N. However, with teflon indenters

secondary radial and cone cracks were sometimes observed at higher loads, leading to segmented fracture outside the contact zone, as previously described in axial testing with harder indenters.²

FEM Stress Analysis

Trajectories (directions of action of stress components) and contours of principal stresses were calculated at specified off-axis loads on the dome inner surface. These stresses have been previously demonstrated to be substantially higher on the inner than the outer surface.¹ The stresses of interest are σ_1 (most tensile) and σ_3 (most compressive). (The intermediate stress σ_2 lies near-normal to the plane of the dome surface, and so is near-zero everywhere.) An example is shown in Figure 5 for indentation on an epoxy-filled glass dome with a balsa disk at 1000 N, viewed from below along the load axis (OZ). The solid lines are contours of the σ_1 principal stress. The first contour indicates zero stress, so that the white central region denotes a compression zone beneath the engulfing indenter. Each contour represents a tensile increment of 10 MPa, amounting to a maximum stress of about 100 MPa at the right margin. The concentration of contours on the right side of the inner surface confirms a strong transfer of stress to the near-side extremities. Note the way these contours extend around the dome base, suggesting that crack initiation could occur anywhere in this region, depending on the availability of starting flaws. Also included in Figure 5 are trajectories of the σ_3 stress component, with an intersection point close to the center of load-

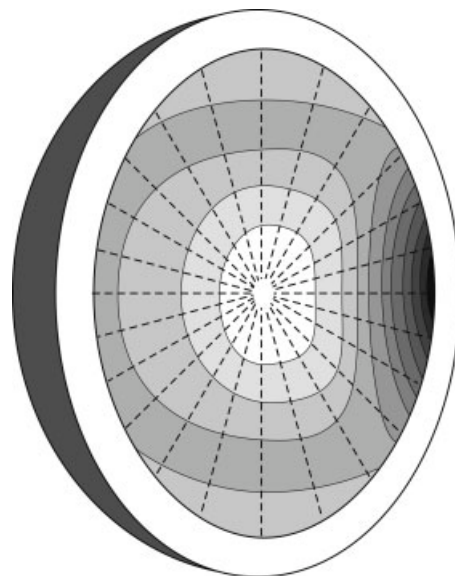


Figure 5. Finite element modeling of principal stresses at inner surface of epoxy-filled glass domes of inner radius 6 mm and thickness 1 mm indented with balsa disk, shown here for load 1000 N. Solid lines are contours of maximum principal stresses σ_1 . Light region indicates compression, dark region tension, each contour is increment of 10 MPa. Dashed lines are trajectories of minimum principal stresses σ_3 . Undersurface view along OZ as in Figure 1(b).

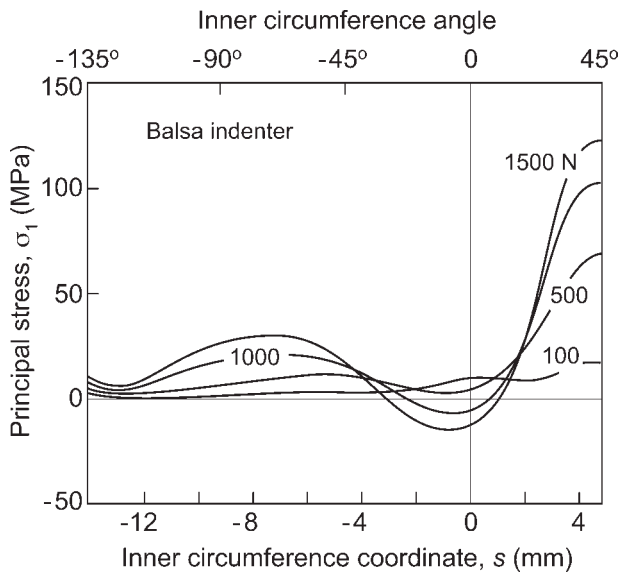


Figure 6. FEM calculations of maximum principal stress σ_1 as function of longitudinal coordinate s measured from contact axis along inner surface, for epoxy-filled glass domes of inner radius 6 mm and thickness 1 mm. Indentation with balsa disk at loads P specified. Note strong buildup of σ_1 in region $s > 0$, and expanding compression zone with load in this region.

ing. Normals to these trajectories indicate the directions of maximum tensile stresses σ_1 , and so indicate approximate crack paths.¹² Note the close correspondence between these trajectories and the crack paths in Figures 2–4.

More detailed stress distributions around the inner surface of the same dome structure are shown in Figures 6 and 7, with σ_1 plotted as a function of longitudinal and latitudinal coordinates s and q , respectively, around the inner dome cir-

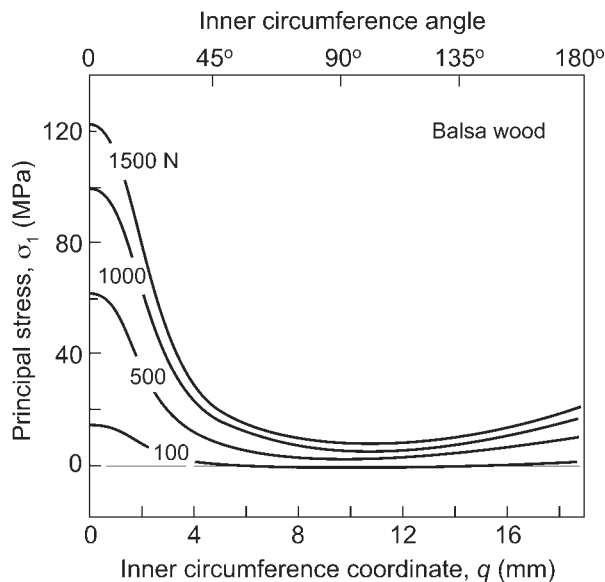


Figure 7. FEM calculations of maximum principal stress σ_1 as function of latitudinal coordinate q measured along inner surface (Fig. 1b), for epoxy-filled glass domes of inner radius 6 mm and thickness 1 mm. Indentation with balsa disk at loads P specified. Note $q = 0$ in this plot corresponds to $s = 45^\circ$ in Figure 6.

cumference (Figure 1), for loads incrementing to 1500 N. Considering the variation with s along the symmetry longitude (i.e., at $q = 0$) in Figure 6 first, we see that the maximum value of σ_1 is at the margin at $s = 45^\circ$, in accordance with Figure 5. This maximum value increases steadily with load but, toward 1000 N, begins to saturate as the compressive engulfment zone spreads across the dome surface. This increasing engulfment is also reflected in the progressive switch in sign of σ_1 at the inner dome surface from tensile to compressive along the contact axis at $s = 0$.

The plot in Figure 7 indicates the distribution of σ_1 with latitude coordinate q around the margin, with $q = 0$ corresponding to $s = 45^\circ$ in Figure 6 and $q = 180^\circ$ likewise corresponding to $s = -135^\circ$. In this case the stress intensities rise steadily with load, and remain tensile around the entire circumference. Note that the stress remains positive with increasing q , consistent with the spread-out contours in Figure 5, so that crack initiation may occur at any point around the margin where uncommonly large starting flaws reside.

Figure 8 plots peak values of σ_1 at the margin $s = 45^\circ$, $q = 0$ as a function of load for the dome system under study here, for off-axis and axial loading using both balsa (solid curves) and teflon (dashed curves) indenters. Note the nonlinearity in the stress/force response for off-axis loading with balsa indenters, attributable to an encroachment of the contact compression zone toward the margins at high loads. Notwithstanding this nonlinearity, the magnifying effect of off-axis loading is clearly evident. The differences in margin stresses between the two indenter materials is not large, suggesting that margin cracks may be initiated by any kind of soft indenter. However, as pointed out earlier, the softer balsa is more effective in suppressing radial cracking in the near-contact zone.¹

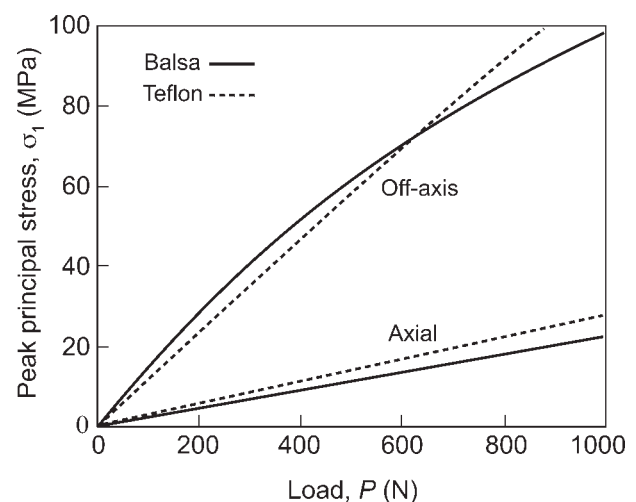


Figure 8. FEM calculations of peak principal stress σ_1 at symmetry margins (i.e., $s = 45^\circ$, $q = 0$) for epoxy-filled glass domes of inner radius 6 mm and thickness 1 mm indented with balsa. Comparing present off-axis data with corresponding data for axial loading from preceding study, for indenters made from balsa (solid curves) and teflon (dashed curves).

DISCUSSION

We have demonstrated how off-axis loading of brittle dome structures with compliant indenters can enhance fracture initiation and propagation from the margins. Unlike the case of axial loading, margin fracture can form from edge flaws without the presence of precursor cracks (i.e., cracks initiated from edge flaws during preparation),^{1,10} because of tensile stress enhancement on the near side. For the off-axis loading considered here, σ_1 reaches its maximum values at the margins, at $s = 45^\circ$, $q = 0$ (Figure 1). In comparison, in axial loading the stress maximum is located on the side face, about two thirds the distance from the load axis to the margins. Fracture paths are governed by the σ_3 radial stress trajectories, that is along paths normal to the maximum tensile stress σ_1 (Figure 5). The ensuing fracture geometry is analogous to the semi-lunar fractures (abfractures) reported in monolithic ceramic crowns.^{5–7}

Data have been obtained using both balsa and teflon indenters. Both materials are compliant relative to typical dental crown materials (tooth enamel and porcelain), and both can lead to the initiation of margin cracks. However, the more compliant balsa is more effective in suppressing radial fractures at the inner dome surface immediately beneath the contact, because of a larger contact at any given load, with attendant engulfing compression zone. Thus while chewing with soft food may dilute local stress intensities, tensile stresses may still be high at the margins, with ensuing margin failures. It is evident from Figure 8 that stresses approaching 100 MPa, that is close to the strengths of typical glass and porcelain materials, may be generated at higher biting loads.

This raises the issue of surface finish. Material strengths may be severely compromised by the introduction of especially large flaws in finishing and preparation operations (e.g. by sandblasting¹³), especially in the margin regions. Such strength loss can lead to a reduction in the corresponding critical load to initiate cracks. This further highlights the need for dental practitioners to avoid such damage in edge preparation of all-ceramic crowns. In the event of a totally uniform distribution of flaws, the favored location for initiation of margin cracks is that of the symmetry position $q = 0$ in Figure 7. However, the presence of larger flaws elsewhere along the margin may shift the initiation site around the circumference, consistent with the observations in Figures 2 and 3. Such lateral shifts may also be caused by nonlinearity in the elastic response of balsa at higher loads,¹ in which case the contact compression zones may be considerably larger than evident in Figures 5 and 6, possibly even extending to the dome edge at very high loads. This could result in suppression of the maxima at $q = 0$ in Figure 7. This could explain why margin cracks tend to initiate nearly symmetrically on opposite side faces, as seen in Figures 2(c) and 3(b).

In view of the propensity to enhanced margin cracking reported in this work, further experimentation with tapered, rounded or chamfered edges could be interesting. Such edges are the norm in dental crown preparation. It would seem that tapered margins might be even more susceptible to fracture, because of enhanced stress concentration. Extension to bilayer crowns consisting of porcelain on a stiff, strong ceramic core might also be a fruitful area of study.

Discussions on semi-lunar fractures with Kenneth Malament at Tufts University are gratefully acknowledged. Certain equipment, instruments or materials are identified in this article to specify the experimental details. Such identification does not imply recommendation by the National Institute of Standards and Technology, nor does it imply the materials are necessarily the best available for the purpose.

REFERENCES

1. Qasim T, Ford C, Bush MB, Hu X, Malament KA, Lawn BR. Margin failures in brittle dome structures: Relevance to failure of dental crowns. *J Biomed Mater Res B* 2007;80:78–85.
2. Kim J-W, Bhowmick S, Chai H, Lawn BR. Role of substrate material in failure of crown-like layer structures. *J Biomed Mater Res* 2007;81B:305–311.
3. McLean JW. The science and art of dental ceramics. Vol. 1: The Nature of Dental Ceramics and Their Clinical Use. Chicago: Quintessence; 1979. pp 39–40.
4. Thompson JY, Anusavice KJ, Naman A, Morris HF. Fracture surface characterization of clinically failed all-ceramic crowns. *J Dental Res* 1994;73:1824–1832.
5. Malament KA, Socransky SS. Survival of dicor glass-ceramic dental restorations over 14 years. I. Survival of dicor complete coverage restorations and effect of internal surface acid etching, tooth position, gender and age. *J Prosthet Dent* 1999;81:23–32.
6. Malament KA, Socransky SS. Survival of dicor glass-ceramic dental restorations over 14 years. II. Effect of thickness of dicor material and design of tooth preparation. *J Prosthet Dent* 1999;81:662–667.
7. Malament KA, Socransky SS. Survival of dicor glass-ceramic dental restorations over 16 years. III. Effect of luting agent and tooth or tooth-substitute core structure. *J Prosthet Dent* 2001;86:511–519.
8. Qasim T, Ford C, Bush MB, Hu X, Lawn BR. Effect of off-axis concentrated loading on failure of curved brittle layer structures. *J Biomed Mater Research* 76B:334–339, 2006.
9. Qasim T, Bush MB, Hu X, Lawn BR. Contact damage in brittle coating layers: Influence of surface curvature. *J Biomed Mater Res B* 2005;73:179–185.
10. Qasim T, Bush MB, Hu X. The influence of complex surface geometry on contact damage in curved brittle coatings. *Int J Mech Sci* 2006;48:244–248.
11. Ford C, Bush MB, Hu XZ, Zhao H. A numerical study of fracture modes in contact damage in porcelain/Pd-alloy bilayers. *Mater Sci Eng A* 2004;364:202–206.
12. Frank FC, Lawn BR. On the theory of Hertzian fracture. *Proc Royal Soc London A* 1967;299:291–306.
13. Zhang Y, Lawn BR, Rekow ED, Thompson VP. Effect of sandblasting on the long-term strength of dental ceramics. *J Biomed Mater Res B* 2004;71:381–386.